

Contents lists available at [SciVerse ScienceDirect](http://www.sciencedirect.com)

Chemosphere

journal homepage: www.elsevier.com/locate/chemosphere

Using slow-release permanganate candles to remove TCE from a low permeable aquifer at a former landfill

Mark D. Christenson^a, Ann Kambhu^b, Steve D. Comfort^{a,*}

^a School of Natural Resources, University of Nebraska, Lincoln, NE 68583-0915, USA

^b Department of Civil Engineering, University of Nebraska, Lincoln, NE 68583-0531, USA

HIGHLIGHTS

- We developed slow-release permanganate-paraffin candles for field scale use.
- We compared two methods of inserting the candles into a low permeable aquifer.
- Laboratory experiments documented candle longevity and radius of influence.
- A pneumatic circulator was developed to facilitate permanganate distribution.
- TCE concentrations in field decreased 67–85% in candle treatment zone.

ARTICLE INFO

Article history:

Received 1 February 2012

Received in revised form 7 June 2012

Accepted 9 June 2012

Available online xxxxx

Keywords:

Permanganate

Chlorinated solvents

TCE

Slow-release oxidants

ABSTRACT

Past disposal of industrial solvents into unregulated landfills is a significant source of groundwater contamination. In 2009, we began investigating a former unregulated landfill with known trichloroethene (TCE) contamination. Our objective was to pinpoint the location of the plume and treat the TCE using in situ chemical oxidation (ISCO). We accomplished this by using electrical resistivity imaging (ERI) to survey the landfill and map the subsurface lithology. We then used the ERI survey maps to guide direct push groundwater sampling. A TCE plume ($100\text{--}600\text{ }\mu\text{g L}^{-1}$) was identified in a low permeable silty-clay aquifer ($K_h = 0.5\text{ m d}^{-1}$) that was within 6 m of ground surface. To treat the TCE, we manufactured slow-release potassium permanganate candles (SRPCs) that were 91.4 cm long and either 5.1 cm or 7.6 cm in dia. For comparison, we inserted equal masses of SRPCs (7.6-cm versus 5.1-cm dia) into the low permeable aquifer in staggered rows that intersected the TCE plume. The 5.1-cm dia candles were inserted using direct push rods while the 7.6-cm SRPCs were placed in 10 permanent wells. Pneumatic circulators that emitted small air bubbles were placed below the 7.6-cm SRPCs in the second year. Results 15 months after installation showed significant TCE reductions in the 7.6-cm candle treatment zone (67–85%) and between 10% and 66% decrease in wells impacted by the direct push candles. These results support using slow-release permanganate candles as a means of treating chlorinated solvents in low permeable aquifers.

© 2012 Elsevier Ltd. All rights reserved.

1. Introduction

The disposal of solid waste into unregulated landfills has resulted in numerous examples of groundwater contamination throughout the United States. Although federal regulations have been enacted to promote safe disposal of nonhazardous waste (e.g., Federal Resource Conservation and Recovery Act, Subtitle D), not all landfills have been in compliance. For example, from 1972 through 1991, small communities in the state of Nebraska with populations of 5000 or less were exempt from solid waste

rules and regulations (NDEQ, 1990). These small landfills were not required to have liners, conduct groundwater monitoring, or take appropriate steps to prevent the disposal of industrial solvents. Although this original exemption was intended to limit the financial burden on small communities, the consequences of not requiring preventative actions have resulted in widespread groundwater contamination. In 1990, Nebraska had 294 unregulated landfills, of which, 135 were identified as having groundwater concerns (Woldt et al., 1998). While many of these solid waste disposal facilities have since closed, several local communities are now strapped with the financial costs of removing industrial solvents such as tetrachloroethene, trichloroethene, and 1,1,1-trichloroethane from their groundwater.

* Corresponding author. Tel.: +1 402 4721502; fax: +1 402 4727904.

E-mail addresses: mdchristenson@huskers.unl.edu (M.D. Christenson), annkambhu@gmail.com (A. Kambhu), scomfort1@unl.edu (S.D. Comfort).

During the past decade, significant efforts have been devoted to developing innovative remedial technologies to treat contaminants at the source. One technology that is relatively mature is the injection of liquid oxidants into contaminated aquifers or in situ chemical oxidation (ISCO) (Watts and Teel 2006). Permanganate is widely accepted as an efficient oxidant for ISCO applications and is extremely efficient in oxidizing chlorinated ethenes to CO₂ (Yan and Schwartz, 1999; Yan and Schwartz, 2000). While the chemistry is sound, the application and delivery of permanganate to the contaminants is still a challenge at many sites. Most ISCO treatments to date have involved injecting oxidants into aquifers as liquids. A common problem with any chemical injection however, is that certain sites have finer textured soils that do not readily accept liquid injections. When this occurs, the chemical oxidant can be observed coming back out of the injection borehole because it offers the path of least resistance. Difficulty in addressing contamination in low permeable soils may be alleviated to some degree by taking a passive approach where a controlled-release oxidant is inserted into the formation and allowed to dissolve and intercept the contaminant over many years.

The idea of encapsulating permanganate for sustained release was first proposed several years ago (Kang et al., 2004; Ross et al., 2005; Schwartz, 2005; Swearingen and Swearingen, 2008) and since then, a number of publications have documented the efficacy of slow-release oxidant dispersal systems to remove chlorinated solvents at the laboratory-scale and in larger flow-tank systems (Lee and Schwartz, 2007a,b; Lee et al., 2008a,b; Lee et al., 2009). Although excellent results have been reported, examples of field-scale applications by practitioners have been limited, in part because commercial sources of slow-release oxidants have not been readily available.

In 2009, we began investigating a former unregulated landfill with known TCE contamination. Our objective was to pinpoint the location of the plume and implement an ISCO remedial strategy. This was accomplished by using a geophysical approach, which characterized the lithology of the landfill and guided groundwater sampling. Because TCE was found to be located in a low permeable aquifer, we hypothesized that using slow-release permanganate candles would be effective at reducing TCE concentrations in the contaminated aquifer. This paper reports the manufacturing and deployment of slow-release permanganate candles (SRPCs) and provides results from both laboratory and field testing aimed at demonstrating the release rates and radius of influence of the SRPCs as well as their efficacy in reducing TCE concentrations.

2. Materials and methods

2.1. Site history and characterization

The former Cozad Solid Waste Disposal Facility is a small community landfill in western Nebraska (Cozad, NE) that operated for 20 yr. During this time, unknown quantities of TCE were deposited into the landfill from residential, commercial, and industrial sources. The facility was closed in 1989 after TCE was detected in monitoring wells located down-gradient from the refuse cells at concentrations above the USEPA's Maximum Contaminant Level (MCL). Remedial attempts to date have included a dual phase extraction facility, poplar tree plantings to induce phytoremediation, and volatilization ponds. Despite these efforts, TCE contamination remains and the migrating plume has not been contained.

To characterize the landfill and identify the location of the plume, several spatial measurements were made. These included: electrical resistivity imaging (ERI, Fig. 1), direct push electrical conductivity logging, hydraulic conductivity measurements and the measurement of soil texture, soil oxidant demand and groundwa-

ter chemistry. Details of these measurements along with chemical standards, and analytical instruments used are provided in supplementary material (in Supplementary Material (SM) SM Section 1.1–1.6, Fig. SM-1).

2.2. Slow-release permanganate candle production

A drying oven (Fisher Scientific-Isotemp Oven 630F), hot plate (Fisher Scientific-Isotemp Hot Plate 11-100-49SH), 6-quart electric skillet and a 2-quart ceramic cooker were preheated to 93 ± 5 °C. Straight solid paraffin wax (Peak Candle Supply-IGI 1343A) was placed into an electric skillet until melted and subsequently transferred to the ceramic cooker to be kept melted and ready for use. Approximately 600 g of KMnO₄ (Carus Corp-RemOxS) were put into glass mason jars and placed into a drying oven to preheat (93 °C) for at least 15–20 min. 250 mL of melted wax was added to an aluminum wax pouring pot and placed on the hot plate. A stand-alone mixer with propeller blade was inserted into the wax, and 600 g of preheated KMnO₄ were quickly added to the melted wax. The mixture was stirred at approximately 2000 rpm until all KMnO₄ particles were blended with the wax. Additional melted wax and/or KMnO₄ was added to the mixture to achieve a mixture with a milkshake like consistency that was just barely pourable. The final ratio by mass of KMnO₄ to paraffin was on average 4.6:1 (w/w). Additional text discussing how the 4.6:1 ratio was chosen is provided in supplementary material (in SM Section 1.7). If the mixture cooled too quickly it was briefly placed back into the drying oven to reheat to 93 ± 5 °C. The mixture was then poured into a 7.6 cm (3 in.) or 5.1 cm (2 in.) by 91.4 cm (36 in.) stock cardboard tube (Yazoo Mills) with a poly tube plug inserted at the bottom. The cardboard tube was gently tamped to remove trapped air bubbles. Once filled, the candle was set aside to cool vertically at room temperature for at least 12 h. Material costs (US\$) per candle (91.4 cm long) were approximately \$18 (5.1-cm dia) and \$40 (7.6-cm dia).

2.3. Laboratory testing of SRPCs

To quantify permanganate release rates and radius of influence, laboratory experiments were conducted with 1.27 cm lengths of the 5.1 and 7.6-cm dia (disc-SRPCs) as well as with miniature candles (mini-SRPCs). The 5.1 and 7.6-cm disc-SRPCs were sealed on the flat top and bottom with a layer of pure wax to ensure diffusion was in the radial direction only, so results could be scaled to any candle length. The miniature candles were prepared in a similar manner to ones used in the field trial but were cast in 0.71-cm dia molds, 2.38 cm in length.

For the mini-SRPCs, we placed individual mini-candles into clear glass jars with 200 mL of deionized water. Sample temperature was maintained at 15 °C and room temperature in two separate experiments. Immediately prior to sampling, the solutions were gently swirled to mix. The solution was sub-sampled via pipette every 10 min for the first hour, hourly for the first 4 h, and approximately daily for the remainder of the experiment. Similarly, the disc-SRPCs were placed in 12.5 L of room temperature deionized water and sub-sampled in the same manner as above with the exception that samples were stirred to mix prior to sampling and collected weekly after the first 10 weeks. Samples were diluted when necessary, and analyzed on a Hach DR 2800 Visual Spectrum Spectrophotometer at 525 nm.

To characterize SRPC performance, we determined temporal KMnO₄ release rates (Flux, *J*) and concentration ratio (*C_r*). Flux was calculated using the following equation.

$$J = \frac{1}{A_{SRPC}} \frac{(C_{n+1}V - C_nV)}{(t_{n+1} - t_n)} \quad (1)$$

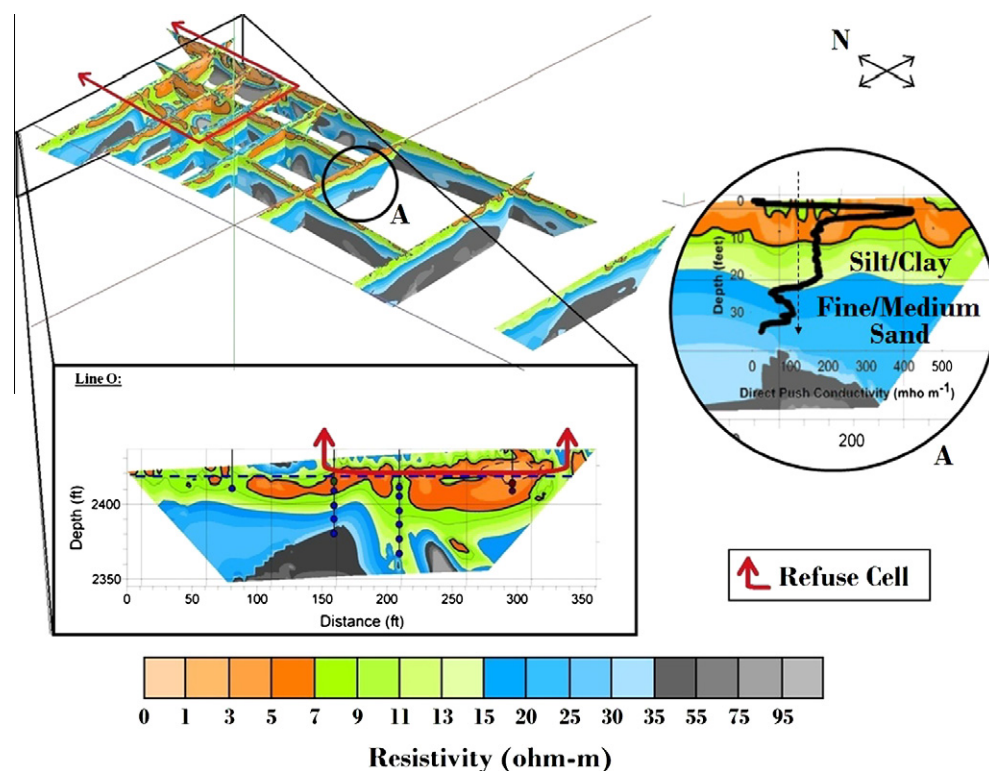


Fig. 1. Composite ERI diagram of the former landfill in Cozad, NE. Figure represents results from 10 of the 19 ERI images obtained. Colored circles in cropped image (Line O) indicates locations and depths from which groundwater samples were obtained and provides an example of how samples were taken from different ERI-identified layers. (A) Results of direct push Electrical Conductivity Survey overlain on Line I in the TCE plume.

where A_{SRPC} is the exposed surface area of the cylindrical SRPC, C_{n+1} the concentration of MnO_4^- in solution at time t_{n+1} , C_n the concentration of MnO_4^- in solution at time t_n , V the volume of the solution, $t_{n+1} - t_n$ is the elapsed time between MnO_4^- measurements. Concentration ratio was calculated using the following equation.

$$C_r = \frac{CV}{M} \quad (2)$$

where M is the initial mass of $KMnO_4$ in the SRPC (Ross et al., 2005). Plots of both J and C_r versus time were fitted using non-linear regression to a 2-parameter power function with SigmaPlot scientific analysis and graphing software. The fitted equations were used to project the performance of the SRPCs with time.

2.3.1. Radius of influence

To ensure the gap between SRPCs at the Cozad field site would be closed, the permanganate radius of influence achievable through diffusion was estimated. Saturated aquifer material collected from sample cores was cut and packed into a $14 \times 14 \times 2.5$ cm 2D tank. A steel cylinder slightly larger than the diameter of the mini-SRPCs was pressed into the low permeable aquifer material to create a pseudo borehole. One mini-SRPC was placed into the bottom of the borehole, sand was poured around the SRPC and the top of the borehole was sealed with bentonite. The saturated tank was then sealed and the diameter of the MnO_4^- distribution was visually observed, measured, and photographed daily. Individual photographs were digitally enhanced with Microsoft Video Editing software (Windows Live Movie Maker) to intensify the color contrast so as to more easily quantify diffusion distances. To estimate the mass of permanganate released from the mini-SRPCs in the 2D tank, a parallel experiment in H_2O was conducted as described in Section 2.3 to determine release rates.

2.3.2. Permanganate distribution from SRPC in sand tank with and without a pneumatic circulator

Fine washed sea sand (VWR) was packed into the same 2D tank described above. A well assembly was fabricated using a 1.6 cm id \times 2.0 cm OD polypropylene tube slotted along 10 cm, starting 2 cm from the bottom of the assembly. The tube was sealed on the bottom and sheathed in fine mesh polyester fabric. The tank was filled with deionized water and the well assembly was centered on the bottom of the tank. Sand was then poured into the tank and allowed to settle under gravity. After the tank was filled with sand, the entire tank was sonicated for 5 min to remove air pockets. Between tests, the tank and well assembly was unpacked, cleaned, and repacked with new sand.

During circulator tests, air was gently bubbled into the water column of the well. Compressed air, supplied by a PETCO AC9903 aquarium air pump, was pumped through a 3.2 mm id \times 6.4 mm OD polyethylene tube connected to a sintered diffusion stone at the bottom of the well assembly. A series of three mini-SRPCs with embedded fishing line were tied to each other and to the diffusion stone to ensure they would remain stationary throughout the experiment. For the non-circulator test, three new mini-SRPCs were suspended at the same depth without a circulator. Migration of the MnO_4^- was observed and recorded in 5 min intervals for the circulator test and daily for the non-circulator test. Additional experiments demonstrating the utility of pneumatic circulator in facilitating permanganate distribution are described in supplementary material (SM Section 1.8).

2.4. Field testing of SRPCs

Treatment of the entire TCE plume was considered impracticable due to the cost to treat the plume in its entirety. Therefore, we installed a permeable reactive barrier (PRB) of permanganate

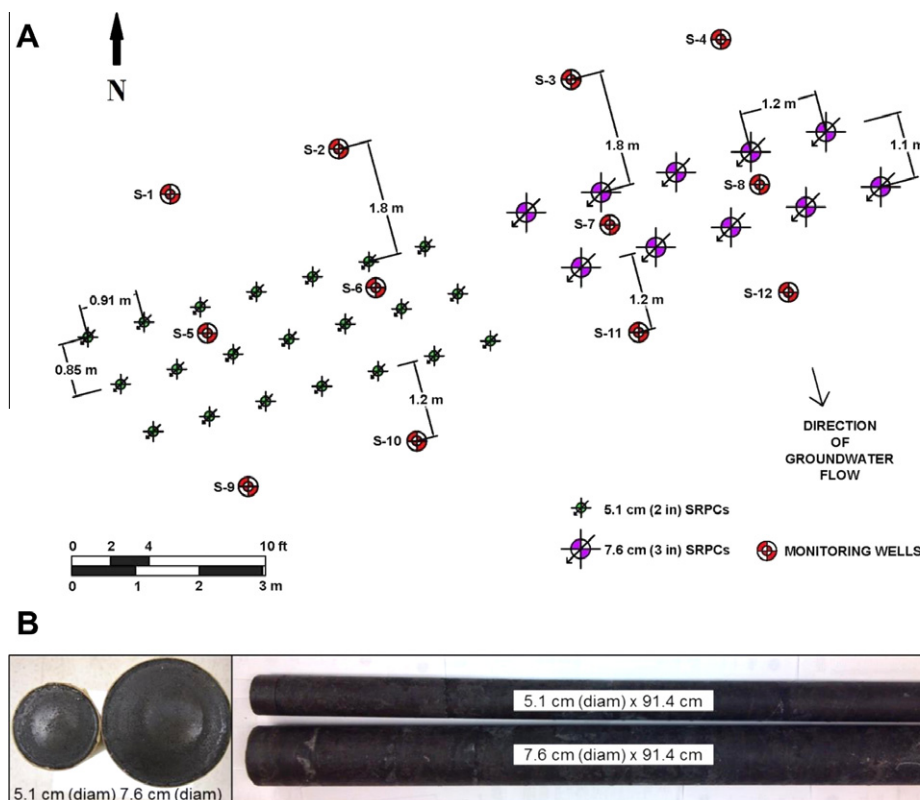


Fig. 2. (A) Field plot of the permeable reactive barrier of SRPCs and monitoring wells; each SRPC location received five candles stack on top of each other; and (B) photograph of permanganate candles.

candles perpendicular to the direction of contaminant flow. Location of the PRB was primarily chosen with the intent to intercept the contaminant plume where TCE concentrations were greatest and the plume was narrow and shallow (Fig. SM-2). Other considerations included choosing a PRB location that was accessible, reasonably level, and up gradient from previously existing monitoring wells.

For comparison, we inserted equal masses of the two diameter SRPCs (50 7.6-cm dia SRPC versus 105 5.1-cm dia) into a low permeable aquifer in staggered rows that intersected the TCE plume. The 7.6-cm candles were placed on 1.2 m centers in two rows while the 5.1-cm candles were inserted via direct push on 0.91 m centers in three rows (Fig. 2, Fig. SM-3). Each SRPC location received five candles stacked on top of each other, covering an aquifer thickness of 4.6 m.

The 7.6-cm SRPCs were removed from cardboard molds and inserted into specially manufactured slotted PVC carriers (Titan Industries, Aurora, NE) and then lowered into 10-cm dia wells. The specially designed tools we used to lower and remove the slotted carriers in and out of the wells are described in supplementary material (Fig. SM-4). In year 2, pneumatic circulators (Fig. SM-5) were placed at the bottom of the 10 wells housing the 7.6-cm SRPCs to improve the distribution of permanganate. Additional details of the procedures used to install the permanganate candles, monitoring wells and sampling and analysis are provided in supplementary materials (SM Section 1.9–1.10).

3. Results and discussion

3.1. ERI and site characterization

Inversion modeling (2D) of ERI data identified four resistivity regions that were assigned different colors for visual interpretation.

These resistivity regions had resistivity measurements (ohms-meter) that ranged from 0 to 7 (orange); >7 to 15 (green); >15 to 35 (blue) and >35 to 95 Ω m (gray) (Fig. 1). The lowest resistivity region (highest electrically conductive region) consisted of a layer beginning at or near the ground surface and was prominent throughout most of the refuse cell (orange layer, Fig. 1). Beneath the orange region was a layer with higher resistivity properties, represented in green (Fig. 1) that intermittently protruded upward into the orange layer creating some discontinuities. The thickest areas of both the orange and green layers were at the highest elevations, near the refuse cell. These layers then decreased moving south and west toward a floodplain near the property boundaries (Fig. 1). Beneath the green layer were two more electrically distinct layers represented by the blue and gray regions. Both layers vary in thickness throughout the site and the gray layer extends beyond the depth of the ERI images (i.e., >16.5 or 22 m).

We found that the ERI survey, soil core analyses, direct push electrical conductivity logging, and slug tests provided complementary results. For example, when ERI images were overlain with direct push electrical conductivity logs, the ERI color regions and EC values match reasonably well (Fig. 1a). Electrical conductivity logging indicated finer sediments in the upper 6 m followed by a transitional region from 6 to 8.2 m. Beneath 8.2 m conductivity values were indicative of coarser sediments. Analysis of soil cores for texture indicated that the orange and green ERI layers were silt loams but between 3 and 7.6 m there was an increase in silt and a decrease in sand content while clay remained relatively constant.

Despite somewhat similar textures among orange and green ERI layers, slug tests from the upper three ERI layers indicated three distinct hydraulic conductivities (Table SM-1). The highest hydraulic conductivity (K_h) was in the blue ERI layer consisting of fine to medium sands as indicated by drilling logs. The average K_h in the blue layer was 20 m d⁻¹. The lowest K_h was in the green ERI layer.

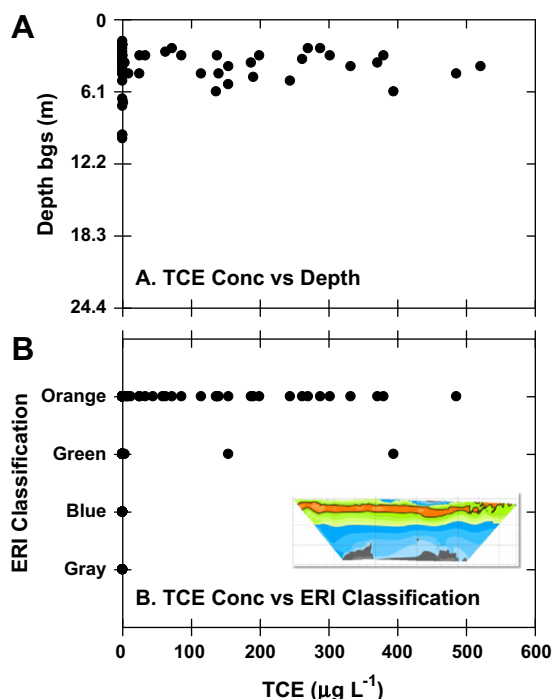


Fig. 3. TCE occurrence in groundwater samples as a function of (A) depth and (B) ERI layer; insert provides example of ERI map.

The average K_h in the green ERI layer was 0.04 m d^{-1} . The orange ERI layer, lying above the green and blue layers in most surveys, had an average K_h of 0.5 m d^{-1} . Slug test results reaffirmed what was observed during manual groundwater sampling where the ease of obtaining water samples from the different ERI regions followed the order of blue (readily obtainable), orange (moderate) and green (difficult).

3.2. Groundwater contamination

Analysis of 146 groundwater samples obtained from 64 sampling locations revealed a distinct relationship between TCE contamination and ERI classifications. Nearly all groundwater samples with detectable TCE (and degradation products) were obtained from the orange ERI layer (Fig. 3). It is important to note that not all groundwater samples obtained from the orange ERI layers were contaminated but the majority of samples with detectable TCE were from the orange regions. TCE was only detected in six samples obtained from the green ERI layer. TCE was not detected in any of the blue and gray ERI layers. Thus, in most cases TCE and its degradation products were located within 6 m of the ground surface (Fig. 3). Coupled with the hydraulic conductivity results, we believe that the low permeable zone below the orange region, represented by the green ERI layer, is acting as an aquitard and preventing TCE transport into the underlying sands.

On a mass basis, more degradation products were present than TCE indicating that natural attenuation was occurring. 1,1-dichloroethene and *cis*-1,2-dichloroethene were the most commonly detected degradation products and present at the highest concentrations. A map of the degradation product detections is presented in supplementary materials (Fig. SM-6). The highest TCE detected at the site was $521 \mu\text{g L}^{-1}$ immediately south of the dual phase extraction facility. From this high point, TCE values decreased along a southeast transect to below the MCL before reaching the southern property boundary (Fig. SM-2).

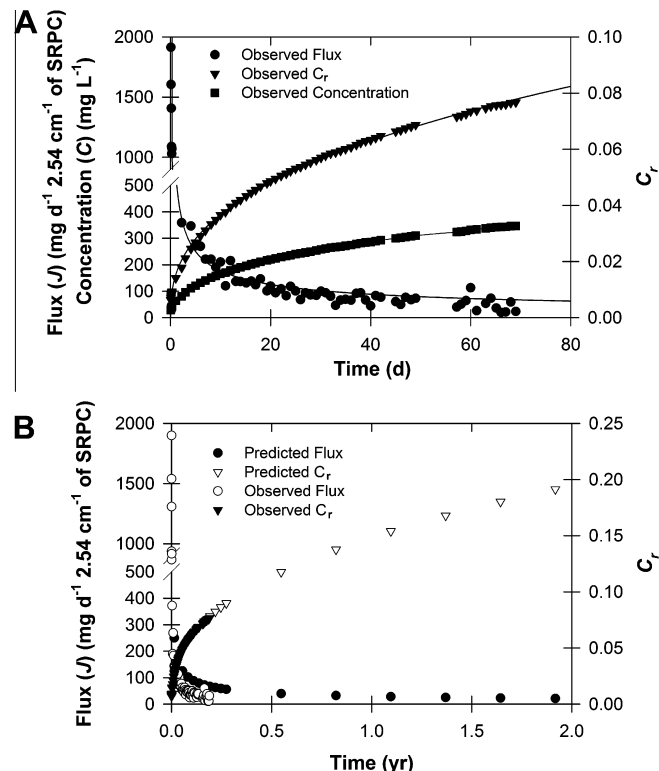


Fig. 4. (A) Observed permanganate concentrations, flux (J ; $\text{mg d}^{-1} 2.54 \text{ cm}^{-1}$ of SRPC) and C_r from disc-SRPCs (5.1-cm dia) in water. (B) Observed J and C_r with values projected out for 2 years.

3.3. SRPC longevity and radius of influence: laboratory results

Two important questions regarding the efficacy of using slow release permanganate candles are: how long will they last? And what is their radius of influence? In an attempt to answer these questions, laboratory experiments were performed with 1.27 cm segments of the candles used in the field (disk-SRPCs) and placed in 12.5 L of H₂O. Chemical dissolution rates from slow-release oxidants can be characterized as an initial flush followed by a slower and sustained release (Kang et al., 2004; Lee and Schwartz, 2007a). Results from the disk-SRPCs showed permanganate concentrations reaching $\sim 200 \text{ mg L}^{-1}$ within the first 10 d and gradually increasing afterward (Fig. 4a). We found these concentrations would be sufficient to remove TCE within a few hours (Fig. SM-7).

Several equations have been used to fit dissolution data to predict longevity. Examples include first-order decay (Lee and Schwartz, 2007b) and power function (Kang et al., 2004). Depending on the equation used, the projected longevity can vary by many years. Attempts at fitting our flux and C_r data to previously used equations also showed considerable variability in projected longevity. For simplicity, we picked 2 years as a timeframe and then predicted flux and C_r from our disk-SRPCs. Results showed a 20.8 mg d^{-1} flux per 2.54 cm of candle length. Also, we project that only $\sim 20\%$ ($C_r = 0.195$) of the 5.1 cm candle would be released after 2 years (Fig. 4).

To determine radius of influence, we inserted mini-SRPC into the low permeable aquifer material (orange ERI region) and then visually measured permanganate distribution. Results showed that within 1 d, the permanganate distribution had a diameter of 3.9 cm (Fig. 5). By dividing the permanganate distribution in half and accounting for the radius of the mini-SRPC (0.355 cm), the permanganate had migrated 1.6 cm beyond the candle after 1 d.

Subsequent measurements showed radius of influences of 3.7 cm after 7 d, 4.6 cm after 14 d and 5.25 cm after 35 d, the time when the majority of the permanganate had been estimated (from parallel experiments, Section 2.3) to be released from the mini-SRPCC (Fig. 5). Scaling results from mini-SRPCs to field SRPC is not straightforward because both candle diameter and permanganate mass differ. Given that diffusion rates are dependent on concentration gradients, it is reasonable to assume that the field-scale SRPCs will impart a greater radius of influence because they can sustain a higher concentration gradient and should not become mass limiting for years as opposed to days for the mini-SRPCs. Actual diffusion distances will also be highly dependent on soil textures, oxidant demand, and groundwater flow rates.

Ultimately, the maximum transverse distances permanganate had to travel through the native aquifer material to close the gaps between the SRPCs used in our field test were 12.7 cm (5.1 cm SRPC) and 17.9 cm (7.6 cm SRPC). In an aquifer with similar properties to the Cozad aquifer, solid fracture emplaced permanganate diffused to create a reactive zone >20 cm (radius) in 10 months (Siegrist et al., 1999). Subsequent diffusion experiments utilizing the same aquifer material yielded a diffusion rate of 0.1 cm d^{-1} over 40 d from a $5000 \text{ mg L}^{-1} \text{ MnO}_4^-$ solution (Struse et al., 2002). When we factored out the early time spike in permanganate flux and late time mass limited flux in our laboratory 2D tank experiments, we calculated a mean diffusion rate of 0.17 cm d^{-1} . Using this estimate for our field site indicated that a minimum of 3–6 months would be needed to close the gaps between candle locations.

While horizontal permanganate migration away from the mini-SRPCs was encouraging in the low permeable material, we also recognized that the 2D tank differed from the field conditions because the direct push 5.1-cm SRPCs were surrounded by a small volume of sand and the 7.6-cm SRPCs were inserted into wells that were not in direct contact with the low permeable aquifer material. With regard to slow release oxidants, the downward migration of permanganate is of greatest concern inside the free water of the

permanent wells (Lee et al., 2008b). When mini-SRPCs were placed directly in water, we observed a steady stream of permanganate migrating down from the candle; similar results were observed in a denser 10% KCl solution (Fig. SM-8). While density driven flow of permanganate has been reported in the past (Lee et al., 2008b), the chemical structure of KMnO_4 also lends itself to intermolecular forces (e.g., dipole–dipole) that are cohesive and cause the molecules to stick together. This cohesiveness can help to exert downward force even in the presence of coarser aquifer material. In 2D tank experiments with sand, we observed uneven permanganate distribution in surrounding media due to sinking of permanganate within the well and out the bottom (Fig. 6). To prevent downward migration, the permanganate molecules need to be separated and solvated so that they can hydrogen bond with H_2O . Consequently, we repeated the 2D tank experiment and for comparison, photographed the migration patterns with and without a pneumatic circulator that emitted small air bubbles to physically break apart the permanganate molecules (Fig. 6).

Permanganate migration patterns from the mini-SRPC alone formed a Christmas tree shape typical of permanganate plumes in sandy media. It took 5 d for permanganate to be visible throughout the majority of the tank. It is clear that the permanganate was accumulating at the bottom of the 2D tank, and stacking its way toward the top. Thus, in a theoretical “bottomless” tank, the treatment zone surrounding the well assembly may never have become adequately treated with permanganate.

Conversely, when small bubbles were emitted from the circulator, an upside-down Christmas tree distribution pattern was observed. Moreover, the time needed to saturate the tank with permanganate was $\sim 75 \text{ min}$, considerably less than the 5 d required without the circulator (Fig. 6). Additionally, the time needed to saturate the treatment zone surrounding the screened interval was only 30 min, and this was the first section of the tank treated instead of the last as observed without the circulator. During subsequent injection tests, circulation of water into the bottom of the well and out the top of the well was clearly evident. Additional

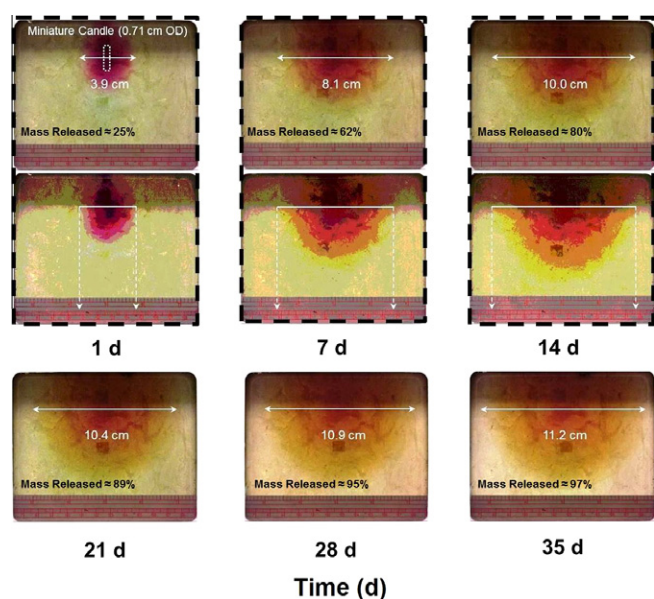


Fig. 5. Temporal changes in diffusion distances (radius of influence) from miniature candles when placed in water-saturated, static, 2-D tank packed with low permeable aquifer material (i.e., orange ERI region). Estimates of mass released were obtained from parallel experiments conducted in H_2O (Section 2.3). Photos with dashed outlines show original photo (top) and digitally enhanced photo (bottom).

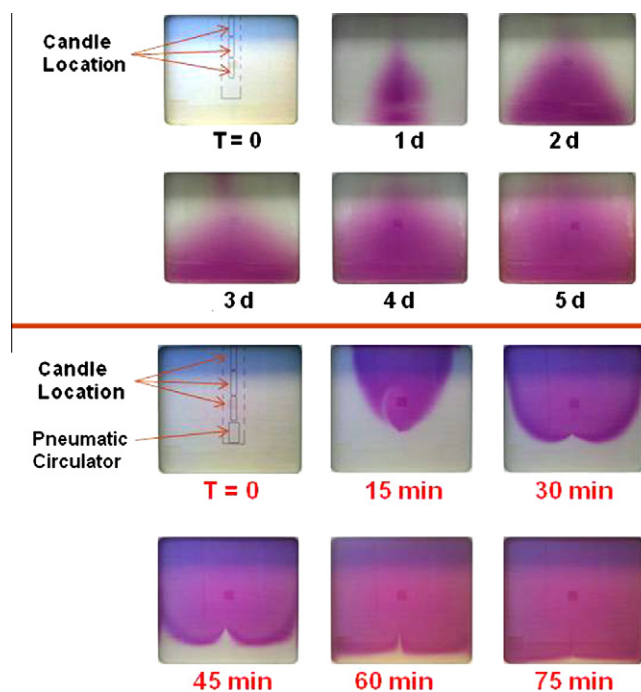


Fig. 6. Temporal changes in permanganate diffusion patterns from three miniature candles placed in water-saturated, static, 2-D tank packed with sand, with and without a pneumatic circulator.

Table 1

TCE concentrations in monitoring wells at Cozad field site. See Figure 2 for location of wells in relation to SRPCs.

Well	Depth (m)	TCE ($\mu\text{g L}^{-1}$)				Well	Depth (ft)	TCE ($\mu\text{g L}^{-1}$)			
		07/25/10	10/10/10	07/06/11	10/13/11			07/25/10	10/10/10	07/06/11	10/13/11
S-1	3.35	378		785	682	S-2	3.35	432		646	582
	5.18			953	701		5.18			642	644
	7.32			814	1209		7.32			1018	632
	AVG			851	864		AVG			769	620
S-5	3.35	469	416	688	835	S-6	3.35	526	477	496	586
	5.18		428	535	517		5.18		506	561	563
	7.32		434	876	544		7.32		532	728	516
	AVG		426	700	632		AVG		505	595	555
S-9	3.35	566		281	298	S-10	3.35	377		549	512
	5.18			290	222		5.18			480	499
	7.32			274	350		7.32			551	531
	AVG			282	290		AVG			527	514
S-3	3.35	215		216	127	S-4	3.35	148		222	82
	5.18			297	132		5.18			240	105
	7.32			284	145		7.32			239	312
	AVG			266	134		AVG			234	166
S-7	3.35	315	396	123	18	S-8	3.35	170	67	123	31
	5.18		13	24	26		5.18		90	24	46
	7.32		24	15	56		7.32		141	15	86
	AVG		145	54	34		AVG		99	54	54
S-11	3.35	371		335	90	S-12	3.35	116		89	22
	5.18			219	142		5.18			93	25
	7.32			193	178		7.32			81	29
	AVG			249	137		AVG			87	26

photographs demonstrating this behavior are provided in supplementary material (Figs. SM-9, SM-10). These data indicate that if SRPCs are placed in porous media, additional measures to control density driven flow would likely be needed.

3.4. SRPC: field results

Monitoring wells were sampled 1 d before (7/25/10) and 77, 346 and 445 d after SRPC installation (Table 1). All wells were sampled with a low-flow sampling technique so as to not artificially accelerate permanganate migration into the monitoring wells (SM Section 1.9). Rather, we wanted the permanganate to diffuse and migrate from SRPCs under natural gradients. Given the low permeability of the aquifer and average linear groundwater velocity ($v = 0.42 \text{ m year}^{-1}$), monitoring wells located 1.2 m down gradient from the SRPCs (wells S-9, S-10, S-11, S-12, Fig. 2) were not expected to show treatment effects for a few years. Similar calculations for the monitoring wells embedded within the SRPC treatment zone (wells S-5, S-6, S-7, S-8, within $\sim 0.5 \text{ m}$ of the SRPCs) indicate travel times of 1.2 years. These travel times however, do not account for the chemical diffusion of permanganate away from the SRPCs and the fact that wells and SRPCs were packed with sand and thus provided more transmissive zones. When monitoring well results were grouped according to the method in which the candles were inserted into the formation (direct push versus permanent wells), results from the first 15 months after installation provided evidence on the effectiveness of SRPC technology.

3.4.1. Field results: direct push candles

Comparisons of TCE concentrations up gradient versus inside the candle treatment zone show some differences (Table 1). For instance, by comparing TCE concentrations in wells S-1 versus S-5 at our last sampling (10/13/11), we observed a decrease of $232 \mu\text{g L}^{-1}$ (26% reduction). Likewise, TCE concentrations in S-6 were $64.6 \mu\text{g L}^{-1}$ lower than S-2. The last two samplings taken out of S-9 (7/6/11 and 10/13/11) were also significantly lower than the initial baseline value (7/25/10) as well as the concentrations up

gradient in wells S-1 and S-5. In fact, TCE concentrations in S-9 represent the lowest values obtained from this set of monitoring wells; specifically, a 66% reduction in TCE concentration over the up gradient well (S-1).

While TCE concentrations in S-5, S-6, S-9, and S-10 are all lower than the up gradient wells (S-1 and S-2), TCE concentrations have not gone down with time. For instance, TCE concentrations in S-5 and S-6 have not decreased temporally and have either stayed similar or increased over the initial baseline values. Part of this can be explained by fluctuations in TCE concentrations coming into the treatment zone (see temporal variations in S-1 and S-2). It is noteworthy that wells S-4 and S-5 are likely only being influenced by one up gradient direct push candle location (see Fig. 2), so any heterogeneity in water flow could cause flow paths to bypass these wells. Monitoring wells S-9 and S-10 on the other hand, have numerous candles (i.e., entire treatment zone) up gradient and may explain the greater reduction in TCE concentrations observed. One potential problem with permanganate is the production of the insoluble MnO_2 , which can cause plugging and flow diversion. This problem however, is generally observed at contaminant and oxidant concentrations that are orders of magnitude higher than those observed in this study. Thus, the candle technology may offer an advantage over liquid injections by providing a sustained release of low concentrations of permanganate.

3.4.2. Field results: candles installed in permanent wells

Incoming concentrations into the permanent well treatment zone were not as high as concentrations observed up gradient of the direct push candle zone. That is, TCE concentrations in monitoring wells S-3 and S-4 have not been as high as S-1 and S-2 (Table 1). Nonetheless, we have observed significant decreases in TCE concentrations in wells S-7 and S-8 with time (i.e., inside treatment zone). TCE concentrations in S-7 and S-8 at our last sampling were significantly lower than initial baseline values and also 67–75% lower than the concentrations in the up gradient wells (S-3 and S-4). Moreover, concentrations in S-11 and S-12 have also decreased with time. As observed in well S-9, TCE concentrations in

the down gradient well S-12, represent the lowest values observed in this set of monitoring wells (an 85% reduction over up gradient well S-4).

Pneumatic circulators were installed in all 10 wells (Fig. SM-5) after the 7/6/11 sampling and results indicate they have influenced TCE removal. TCE concentrations in wells S-7, S-8, S-11 and S-12 all decreased from 7/6/11 to 10/13/11. Prior to installation, density driven flow of permanganate appeared to be causing more of a decrease in TCE concentrations in S-7 at the lower depths (7.32 versus 3.35 m); this was also supported by measured permanganate concentrations. After installing the circulators, TCE concentrations were lower at the 3.35 m elevation rather than the deeper depths; this was also observed in well S-11 (Table 1). It is also noteworthy that we visually inspected the 7.6-cm candles 428 d after installation (9/26/11) by removing them from the wells and carriers. Candles were mainly intact and showed very little deterioration but some had an oxidized manganese coating, which we quickly removed with a hand wood planer before reinserting. Whether this refurbishing is needed on a routine basis (i.e., annual or biennial) has yet to be determined but this option is available when candles are placed in wells as opposed to direct push.

While the characteristics of the low permeable aquifer at the Cozad site dictates that additional field monitoring will be needed for several years to fully determine the efficacy of the slow release candles, initial field results and the supporting laboratory results presented indicate that slow-release permanganate candles may be an effective means of treating chlorinated solvents in low permeable zones. Potential advantages to the candle technology are that they negate the need for specialized equipment (mixing trailer, pumps, hoses, etc.), curtail health and safety issues associated with handling liquid oxidants, and when used in a barrier design, could potentially provide a long-term solution for controlling contaminant migration.

Acknowledgments

The authors greatly acknowledge the technical assistance of Matt Marxsen and the University of Nebraska Conservation and Survey Division for well installation and sampling. Appreciation is expressed to the Nebraska Department of Environmental Quality and the City of Cozad, NE for assisting with field site logistics. We also thank Dr. Todd Halihan and Aestus LLC, for their technical assistance with ERI measurements. Additionally, we thank Napatsawan Noi Wong for her assistance with the GIS plume contouring. Funding was provided in part by EPA Region 7, Project ER-0635.

Partial support was also provided the University of Nebraska School of Natural Resources and Water Science Laboratory. This paper is a contribution of Agricultural Research Division Projects NEB-38-071.

Appendix A. Supplementary material

Supplementary data associated with this article can be found, in the online version, at <http://dx.doi.org/10.1016/j.chemosphere.2012.06.009>.

References

- Kang, N., Hua, I., Rao, P.S., 2004. Production and characterization of encapsulated potassium permanganate for sustained release as an in situ oxidant. *Ind. Eng. Chem. Res.* 43, 5187–5193.
- Lee, B.S., Kim, J.H., Lee, K.C., Bin Kim, Y., Schwartz, F.W., Lee, E.S., Woo, N.C., Lee, M.K., 2009. Efficacy of controlled-release KMnO_4 (CRP) for controlling dissolved TCE plume in groundwater: a large flow-tank study. *Chemosphere* 74, 745–750.
- Lee, E.S., Liu, G.M., Schwartz, F.W., Kim, Y.J., Ibaraki, M., 2008a. Model-based evaluation of controlled-release systems in the remediation of dissolved plumes in groundwater. *Chemosphere* 72, 165–173.
- Lee, E.S., Schwartz, F.W., 2007a. Characteristics and applications of controlled-release KMnO_4 for groundwater remediation. *Chemosphere* 66, 2058–2066.
- Lee, E.S., Schwartz, F.W., 2007b. Characterization and optimization of long-term controlled release system for groundwater remediation: a generalized modeling approach. *Chemosphere* 69, 247–253.
- Lee, E.S., Woo, N.C., Schwartz, F.W., Lee, B.S., Lee, K.C., Woo, M.H., Kim, J.H., Kim, H.K., 2008b. Characterization of controlled release KMnO_4 (CRP) barrier system for groundwater remediation: a pilot-scale flow-tank study. *Chemosphere* 71, 902–910.
- Nebraska Department of Environmental Quality (NDEQ). 1990. Groundwater quality investigation of five solid waste disposal sites in Nebraska. In: Nebraska Department of Environmental Quality, February. Lincoln, NE.
- Ross, C., Murdoch, L.C., Freedman, D.L., Siegrist, R.L., 2005. Characteristics of potassium permanganate encapsulated in polymer. *J. Environ. Eng.* 131, 1203–1211.
- Schwartz, F.W., 2005. Semi-Passive, Chemical Oxidation Schemes for the Long-term Treatment of Contaminants. The Ohio State University, Columbus, OH.
- Siegrist, R., Lowe, K., Murdoch, L., Case, T., Pickering, D., 1999. In situ oxidation by fracture emplaced reactive solids. *J. Environ. Eng.* 125, 429–440.
- Struse, A., Siegrist, R., Dawson, H., Urynowicz, M., 2002. Diffusive transport of permanganate during in situ oxidation. *J. Environ. Eng.* 128, 327–334.
- Swearingen, J., Swearingen, L., 2008. Patent No. US 7,431,849 B1, Encapsulated Reactant and Process. United States of America.
- Watts, R.J., Teel, A.L., 2006. Treatment of contaminated soils and groundwater using ISCO. *Pract. Periodical Haz., Toxic, Radioact. Waste Manage.* 10, 2–9.
- Woldt, W.E., Hagemaster, M.E., Jones, D.D., 1998. Characterization of an unregulated landfill using surface-based geophysics and geostatistics. *Ground Water* 36, 966–974.
- Yan, Y.E., Schwartz, F.W., 1999. Oxidative degradation and kinetics of chlorinated ethylenes by potassium permanganate. *J. Contam. Hydrol.* 37, 343–365.
- Yan, Y.E., Schwartz, F.W., 2000. Kinetics and mechanism for TCE oxidation by permanganate. *Environ. Sci. Technol.* 34, 2535–2541.